Nanoscale

Accepted Manuscript

This article can be cited before page numbers have been issued, to do this please use: H. Wang, H. Sui, Y. Zheng, Y. Jiang, Y. Shi, J. Liang and L. Zhao, *Nanoscale*, 2019, DOI: 10.1039/C9NR01255A.

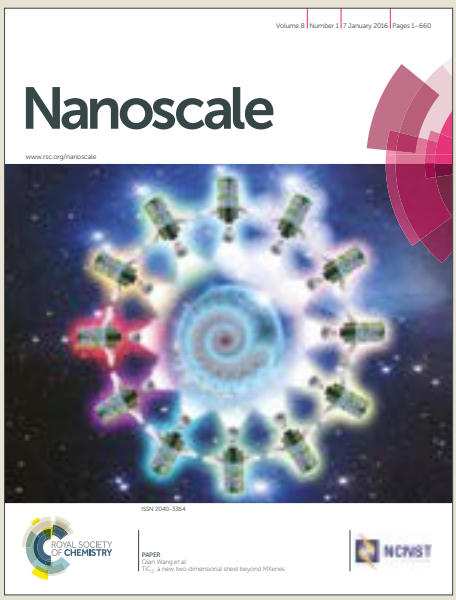

ROYAL SOCIETY OF CHEMISTRY

rsc.li/nanoscale

View Article Online
DOI: 10.1039/C9NR01255A

Curcumin-primed exosomes potently ameliorate cognitive function in AD mice by inhibiting hyperphosphorylation of Tau protein through the AKT/GSK-3β pathway

Hao Wang[1a], Haijuan Sui[2a], Yan Zheng[1], Yibing Jiang[1], Yijie Shi[1*], Jia Liang[3*], Liang Zhao[1*]

1 School of Pharmacy, Jinzhou Medical University, Jinzhou 121000, P R China;

2 Department of Pharmacology, Jinzhou Medical University, Jinzhou, 121000, P R China;

3 Life Science Institution, Jinzhou Medical University, Jinzhou, P R China;

*Corresponding author, email: shiyijie119@163.com (Yijie Shi); liangjia@jzmu.edu.cn (Jia Liang); liangzhao79@163.com (Liang Zhao)

Tel: +86 (0)416 4673430, Fax: +86 (0)416 4673439

[a] These two authors contributed equally to the manuscript

Email addresses:

HW: jzmuwanghao@163.com

HS: shj305506@163.com

YZ: lyyxzhengyan@163.com

YJ: 850095332@qq.com

YS: shiyijie119@163.com

JL: liangjia@jzmu.edu.cn

LZ: liangzhao79@163.com

View Article Online
DOI: 10.1039/C9NR01255A

Abstract

Alzheimer's disease (AD) is a progressive development of fatal neurodegenerative diseases. Owing to the unclearness of pathogenesis of AD and failure of drug on crossing the blood-brain barrier (BBB), currently there is a lack of effective diagnostic and therapeutic approaches in the treatment of AD. The aim of this study was to design exosomes (Exo) as a specifically-designed carrier able to carry curcumin (cur) for preventing neuronal death in vitro and in vivo to alleviate AD symptoms. Our results demonstrated that Exo improved solubility and bioavailability of cur as well as increased drug penetration across the BBB by specific active targeting between Exo inherited the lymphocyte function-associated antigen 1 (LFA-1) and endothelial intercellular adhesion molecule 1 (ICAM-1). Exosomes derived from curcumin-treated (primed) cells (Exo-cur) can better prevent the death of neurons in vitro and in vivo to relieve the symptoms of AD by inhibiting phosphorylation of Tau protein through activating AKT/GSK-3β pathway. Our results suggested that Exo-cur featured highly effective BBB-crossing via receptor-mediated transcytosis to access brain tissues and inhibited Tau phosphorylation, holding great potentials on improving drug targeted delivery and recovery of neuronal function in the AD therapy.

Keywords: Alzheimer's disease, blood-brain barrier, exosomes, curcumin, Tau

Introduction

Alzheimer's disease (AD) is a neurodegenerative disease with insidious and

View Article Online
DOI: 10.1039/C9NR01255A

progressive onset of disease. Its clinical manifestations include progressive memory loss, cognitive dysfunction, executive dysfunction and behavioral changes[1]. Although the etiology and pathogenesis of AD have not been elucidated, accumulated evidences show that AD is associated with extracellular inflammatory plaques (NPs/senile plaques, SPs) formed by the deposition of amyloid-beta protein (Aβ) and neuronal fiber tangles in neuronal cells formed by phosphorylated Tau protein [2-4].

In the past few years, based on targeted Aβ, researchers tried to find effective drugs to inhibit the production and aggregation of Aβ proteins or promote its clearance. However, these drugs failed to reverse AD or delay progression. Especially, the failure of Aβ monoclonal antibodies solanezumab and bapineuzumab in phase III clinical trials questioned the validity of Aβ as a therapeutic target [5-7].

Nowadays, more researchers switch their interests on inhibition of phosphorylation and aggregation of Tau as a major therapeutic target [8-10]. It was found that over activation of GSK-3β increased the Tau hyperphosphorylation (Ser-396 sites), thus resulting in the formation of neurofibrillary tangles (NFTs) and depolymerization of the microtubules, further causing a series of cellular metabolic disorders and affecting the transport of substances between axons and dendrites [11-13]. Therefore, this mechanism provides us to find an effective drug to inhibit GSK-3β-mediated phosphorylation of Tau protein, thereby alleviating and even treating Alzheimer's disease.

Apart from finding a new potential target to treat AD, it is also important to seek a strategy to assist drugs across the blood-brain barrier (BBB) and achieve intracranial

View Article Online
DOI: 10.1039/C9NR01255A

drug delivery. The existence of BBB greatly hinders the penetration and accumulation of chemotherapeutics into brain, accompanied by poor therapeutic effects. Overall, only high-fat soluble substances with molecular weights below 400 Da are allowed to pass through BBB. However, more than 98% drugs molecules are unable to meet these harsh requirements [14-17]. In order to enhance intracranial drug delivery, various methods such as surgery, inputting hyperosmotic liquid and chemical modification of drugs are applied to open BBB and increase the intracranial amount of drugs. Unfortunately, the disadvantages such as brain infection risk, the non-specific absorption through the whole body and unexpected toxicity of drugs to normal organs were inevitably appeared. Therefore, developing an elaborate strategy to achieve simultaneous BBB-crossing for AD treatment, is of great significance.

Exosomes (Exo) as cell-derived bilayer lipid vesicles with a diameter of 40-100 nm, are mainly reported on information exchange and substance transfer between cells [18-20]. Recently, it is also considered to be a desirable drug delivery vehicle owing to its excellent characterization [21-23]. Like cell membrane, Exo has a lipid bimolecular structure, which provides the possibility for Exo to efficiently load hydrophobic and hydrophilic drugs[24-25]. As Exo is widely found in humans, such as blood, urine, and cerebrospinal fluid, it may be low immunogenic and has a longer circulating half-life in the human body[26-27]. Furthermore, some peptides inherited by Exo could specifically combine with its receptor in targeted cells, thus accelerating the accumulation of Exo in targeted tissues[28]. Therefore, Exo showed the targeted ability when delivering drugs through ligand-receptor-mediated active targeting process.

View Article Online
DOI: 10.1039/C9NR01255A

It was reported that curcumin, 1,7-bis-(4-hydroxy-3-methoxyphenyl)-1,6-heptadiene-3,5-dione, is a diarylheptanoid, belonging to the group of curcuminoids. Additionally, curcumin has a simple structure with two phenolic functional groups connected by a conjugated b-diketone system and exhibits the regulation of Tau phosphorylation[29]. Based on the previous report on treatment of AD with cur from the perspective of the regulation of Tau phosphorylation [30-31], we aim at investigating effect of cur on the regulation of Tau phosphorylation from the molecular levels. To overcome the above problems associated with the solubility and bioavailability of cur, we fabricated curcumin-primed exosomes (Exo-cur) secreted by cur treated mouse macrophage cells to improve its solubility, stability and tissue bioavailability. Exo inherited the lymphocyte function-associated antigen 1 (LFA-1) from their parental cells, a protein that interacts with endothelial intercellular adhesion molecule 1 (ICAM-1), mediates the lateral migration and diapedesis of Exo across the BBB [32-33], we hypothesized that Exo-cur can effectively penetrate BBB and transfer more proportions of cur into brain (Fig. 1). We used okadaic acid (OA) to induce Tau hyperphosphorylation and establish an animal model of AD [34-36], and evaluated the beneficial role of Exo-cur by inhibiting OA-induced phosphorylation of Tau. The effect of Exo-cur on attenuating OA-induced learning and memory deficits was also investigated in OA-induced Tau-phosphorylated AD-like mouse model and explored its neuroprotective effects by inhibiting AKT/GSK-3β mediated Tau phosphorylation.

Fig. 1 The primary hypothesis of this study. Exosomes derived from curcumin-treated (primed) cells (Exo-cur) can better relieve the symptoms of AD by inhibiting phosphorylation of Tau

View Article Online
DOI: 10.1039/C9NR01255A

protein through AKT/GSK-3β pathway. Exo-cur secreted by cur treated RAW 264.7 was collected and purified by ultracentrifugation. The safe and effective delivery of cur across the blood–brain barrier (BBB) due to the interaction between Exo inherited LFA-1 and endothelial ICAM-1 was demonstrated in vivo and in vitro. Furthermore, Exo-cur inhibited OA-induced phosphorylation of Tau and ameliorated cognitive function in AD mice. It demonstrated that the novel Exo-cur had a target treatment capability for AD and can traverse the BBB, indicating the potential for the effective treatment of AD.

Experimental

Cell culture

The macrophage cell line, RAW 264.7 (mouse leukemic monocyte macrophage cell line), and the brain microvascular endothelial cell line (hCMEC/D3), which served as a model of the human BBB, were established by the Shanghai Institute of Cell Biology, Chinese Academy of Sciences, Shanghai (People's Republic of China). Murine macrophage RAW264.7 cell line was cultured in Dulbecco's modified Eagle's medium (DMEM, Hyclone, UT, USA) containing 10% fetal bovine serum (FBS; Gibco, CA, USA) and 1% penicillin-streptomycin (PS). The hCMEC/D3 was cultured in Dulbecco's Modified Eagle Medium: Nutrient Mixture F-12 (DMEM/F-12) supplemented with 10% fetal bovine serum (FBS) and 1% PS.

Animals

Healthy adult male SD rats aged 7–8 weeks and weighing 200 ± 18 g were purchased from Beijing Vital River Laboratory Animal Technology Company and kept in the thermo-regulated, humidity-controlled condition under a 12 h day/night light cycle

View Article Online
DOI: 10.1039/C9NR01255A

provided by the experimental and feed with standard rat chow and water ad libitum. C57BL/6 mice (Beijing Vital River Laboratory Animal Technology Co., Ltd) at age 5 to 7 weeks were raised in the Animal Center of Jinzhou Medical University. Mice were housed in groups of four or five per cage and maintained under standard laboratory conditions (temperature 24 ± 1 °C, humidity 60 – 70%, 12-h light – dark cycle) with free access to food and water. One-week rearing was required for acclimating to the new environment and mice were used for study at the age 6 to 8 weeks. All animals were handled in strict accordance with the Animal Ethics Procedures and Guidelines of the People's Republic of China, and this study was approved by the Animal Ethics Committee of Jinzhou Medical University.

Induction of AD model in vivo

Stereotaxic injection with OA on one side of hippocampal area was applied to C57BL/6 mice for constructing the animal model of AD [37]. The mice were anesthetized with 2% isoflurane and fixed to the stereo positioning device (RWD life Science Co., ltd., shenzhen, china). According to a mouse brain stereotaxic atlas, the skull of mouse was opened followed by drilling holes in the area of the right ventral hippocampus (front and rear: -2.18 mm, medial: -1.5 mm, dorsal abdomen: -1.8 mm). 2 μL of OA (0.2 μM; Upstate Biotechnology, Inc., Lake Placid, NY, USA) dissolved in dimethyl sulfoxide at 1 μM and diluted to 0.2 μM in artificial cerebrospinal fluid was injected the right dorsal hippocampus. The injection continued for 5 minutes, and had the injector needle after the injection to keep the home position 2 minutes to guarantee the complete infusion medicine. After that, the mice were treated with

View Article Online
DOI: 10.1039/C9NR01255A

penicillin and allowed to recover from surgery under the daily monitoring of body weight, food and water intake. After 5 days, the mice were randomly and equally divided into five groups (n = 3 per group) as follows: (1) Sham group: mice in the normal control group received a daily peritoneal injection of 0.2 mL saline for consecutive 7 days. (2) OA group: OA treated mice received a daily peritoneal injection of 0.2 mL saline for consecutive 7 days. (3) OA+cur group: OA treated mice received a daily peritoneal injection of 0.2 mL saline suspension of cur at 100 μg/mL of cur for consecutive 7 days. (4) OA+Exo-cur group: OA treated mice received a daily peritoneal injection of 0.2 mL saline suspension of Exo-cur at 100 μg/mL of cur for consecutive 7 days. (5) OA+Exo group: OA treated mice received a daily peritoneal injection of 0.2 mL saline suspension of Exo for consecutive 7 days.

Curcumin-primed exosome collection and characterization

The toxic activity of cur on macrophage RAW264.7 cell was determined in a 24 hour MTT (3-(4,5-dimethyl-2-thiazolyl)-2,5-diphenyl-2-H-tetrazoliumbromide) assay (cytotoxicity test) and we found that the cell viability of cur was not significantly decreased at all concentrations, ranging from 5 to 40 μg/mL, and more than 80% of cells survived. Based on these results, macrophage RAW264.7 cells were treated with cur (40 μg/mL) for 24 h. Culture media was collected and centrifuged at 3,000 rpm (10 min) and supernatant was collected. Collected supernatant was further ultracentrifuged at 1,00,000 rpm (1 h) to concentrate Exo-cur in pellet. The characterizations of Exo and Exo-cur were determined using characterized by a transmission electron microscope (TEM) (JEM-1200EX; JEOL, Tokyo, Japan) and

View Article Online
DOI: 10.1039/C9NR01255A

atomic force microscopy (AFM) (FM-Nanoview6800; FSM-PRECISION, Suzhou, China). Particle size and surface charge were measured by dynamic light scattering (DLS) (Zetasizer Nano ZS; Malvern Instruments, Malvern, UK). The amount of cur loaded into Exo was measured by dissolving Exo-cur with methanol to release cur and the content of cur in Exo was determined by detecting fluorescence absorbance of cur, which is excited at 425 nm and emitted at 530 nm using a fluorescence spectrophotometer (F-4600, Hitachi, Tokyo, Japan). Loading capacity and encapsulation efficiency of cur were calculated using the following formulation and exosomal proteins were analyzed by BCA method.

$$EE\% = \frac{W_0}{W_1} \times 100\% \qquad (1)$$

$$LC\% = \frac{W_0}{W} \times 100\% \qquad (2)$$

W_0 was the weight of cur enveloped in Exo, W was the weight of Exo-cur, and W_1 was the initial amount of cur added in the culture medium.

To access the release of free cur and Exo-cur in vitro, cur and Exo-cur containing 20 μg cur were solubilized in 1mL phosphate buffer solution (PBS, pH 7.4, 37°C) containing 0.5% carboxymethyl cellulose (CMC) and added into the dialysis bag with a molecular weight cutoff of 2,000 molecular weight (Mw), then the dialysis bag was immersed in a flask containing 200 mL of release medium (pH7.4, phosphate buffer solution, 37°C) and 0.5% (w/v) anionic surfactant sodium dodecyl sulfate (SDS). Samples were taken at time points from inside the flask and the amount of released cur was analyzed by detecting fluorescence absorbance of cur, which is excited at 425

View Article Online
DOI: 10.1039/C9NR01255A

nm and emitted at 530 nm.

In vitro solubility and stability assays

To determine enhanced solubility of cur with the encapsulation of Exo, excessive cur and exosomal cur were added to 2 ml PBS (pH 7.4) and incubated in the dark in a 37 °C water bath under the stirring for 30 min followed by centrifugation at 15,000 rpm for 15 minutes. The supernatant was collected and filtered through a 0.45 μm Millipore filter (EMD Millipore, Billerica, MA, USA) and the maximum solubility of free cur and Exo-cur was determined by described fluorescence spectrophotometry method above. Comparison of stability between free cur and Exo-cur were investigated by incubating cur and exosomal cur at same concentration of 1.5 μg /mL at 2 ml PBS (pH 7.4) and plasma in the dark in a water bath at 37 °C and determine the concentration of cur at different time points. We took fluorescence absorbance value of cur or exosomal cur at the beginning as the control group (100%) and the remaining ratio (RR) of cur or exosomal cur were calculated using the following equation:

$$RR\% = \frac{A\mathrm{b}_t}{A\mathrm{b}_0} \times 100\%$$

$A\mathrm{b}_t$ was fluorescence absorbance value of cur or exosomal cur at predetermined time, $A\mathrm{b}_0$ was fluorescence absorbance value of cur or exosomal cur at the beginning.

Pharmacokinetic studies in SD rats

The tissue distribution and bioavailability of free-cur and Exo-cur in SD rats were performed following our previous publication [38]. Briefly, the rats were randomly divided into two groups (n=3), namely, free-cur and Exo-cur, then weighed and i.v.

View Article Online
DOI: 10.1039/C9NR01255A

administered a single dose of various cur formulations at 0.4 mg/kg. Blood samples were periodically collected via eye sinus bleeding and immediately centrifuged to obtain plasma for determining cur content. At 24 h after dosing, all the animals were euthanized and tissues were immediately dissected out and homogenized for extracting cur. For histological examination, the paraffin-embedded sections of the organs of rats were sliced (5 μm) and then HE staining for light microscope observations was performed.

To further monitor the distribution of free-cur and Ex-cur in brain, C57BL/6 mice were randomly divided into two groups (n=3), namely, free-cur and Exo-cur, then weighed and intraperitoneal administered a single dose of various cur formulations. At 6 h and 24 h, the brain of mice were dissected and an IVIS Spectrum imaging system (PerkinElmer, Waltham, MA, USA) was employed to capture cur emitted fluorescence images of brain. The cur-related fluorescence signals were discriminated from the auto-fluorescence signals using Living Image software (PerkinElmer).

In vitro cellular uptake

In order to further explore the intracellular internalization and distribution of free-cur and Exo-cur, they were incubated with hCMEC/D3 cells in the culture medium containing free ICAM-1 or no ICAM-1 for a certain period of time. The nucleus was stained with Hoechst (blue) for 15 min at 37 °C. At predetermined intervals, the cellular distributions of free-cur and Exo-cur were observed by confocal laser scanning microscopy and was quantified using a microplate reader (Synery-2; BioTek Instruments, Winooski, VT, USA) by checking the fluorescence intensity of cur,

View Article Online
DOI: 10.1039/C9NR01255A

which is excited at 425 nm and emitted at 530 nm.

Penetration study using an in vitro BBB model

A monolayer transwell culture using the brain microvascular endothelial cell line, hCMEC/D3, is a common in vitro BBB model that is used to study the brain delivery of cur. The hCMEC/D3 cell mix (in 0.5–1.0 mL of total volume) was added into the insert filled with serum free medium containing free ICAM-1 or no ICAM-1 in the upper chamber of a 12-well transwell plate for monolayer cell culture with a transendothelial electrical resistance >300 Ω; PBS at a pH level of 7.4 was added into the lower chamber. The suspensions of free-cur and Exo-cur were placed in the upper chamber for continuous incubation in an incubator set at 37°C, 5% CO_2. Afterward, free-cur and Exo-cur were transferred across the cells and entered the lower chamber. The quantification of the penetrated cur in the lower chamber was detected using a microplate reader (Synery-2; BioTek Instruments, Winooski, VT, USA) by checking the fluorescence intensity of cur, which is excited at 425 nm and emitted at 530 nm. The relative fluorescence ratio (RFR, %), which represents the penetration rates of cur, was calculated by determining the ratio of the fluorescence intensity of the penetrated cur in the lower chamber to that of the initially added cur in the upper chamber.

Morris Water Maze test

The spatial learning and memory of mice were accessed by Morris Water Maze test**.** After 5 days of OA injection, 0.2 mL saline, saline of Exo and the saline suspensions of cur and Exo-cur containing 100 μg/mL of cur were administered via a single peritoneal injection daily for consecutive 7 days. After that, mice were placed in a

View Article Online
DOI: 10.1039/C9NR01255A

circular pool (120 cm in diameter; height 40 cm; aqueous 22±2℃) in which four equal interval quadrants were allocated and translucent platform (8 cm x8 cm) was placed in the center of quadrant and immersed 1 cm below the surface of the water. Each mouse is allowed to swim in a circular pool filled to a depth of 30 cm with water made opaque with white non-toxic water-based tempura paint. The platform remained in the same position throughout the learning trials and visual cue tests. In the initial guided learning days, maximum swim time was set to 90 s. If the mouse located the platform before 90 s had passed, it was immediately removed from the pool. If the platform was not located after 90 s of swimming, the mouse was gently guided to the platform and allowed to re-orient to the distal visual cues for an additional 15 s before being removed from the pool. The swimming escape incubation period was recorded throughout the learning trials and visual cue tests. During the probe test, the platform was removed from the pool, the time spent in the target quadrant and the number of times the animal crossed the platform's previous position were recorded through the video tracking system.

Immunofluorescence staining

Frozen sections of brain tissue were fixed in cold acetone (pre-cooled in a refrigerator at -20 °C in advance) for 10 min and washed three times with PBS for 5 min each time. After covering with 3% BSA for 1 h at room temperature， the brain section was co-incubated with 100 μL of primary antibody（1:500）for overnight at 4 °C followed by washing three times with PBS for 5 min each time. Next, 100 μL of anti-mouse fluorescent secondary antibody at a ratio of 1:500 was added and

View Article Online
DOI: 10.1039/C9NR01255A

incubated at room temperature for 1 h in the dark. After washing 3 times by PBS, staining by DAPI, and mounting with ProLong Antifade Reagents (Invitrogen), the tissue slides were imaged by a FV10i confocal microscope (Olympus, Tokyo, Japan). Images were processed and analyzed by ImageJ software (NIH). All settings of imaging and processing were kept constant, and the relative fluorescence intensities were calculated.

Protein extraction in brain tissue and western blot analysis

The brain tissue samples were quickly washed three times with cold phosphate-buffered saline and then homogenized in ice-cold RIPA buffer containing 2 mM phenylmethanesulfonyl fluoride (PMSF), phosphatase inhibitors and protease inhibitor cocktail. The protein in the supernatant was collected by centrifugation and determined by the BCA assay. After being separated through 10% sodium dodecyl sulfate polyacrylamide gel electrophoresis, protein was transferred onto polyvinylidene fluoride membrane. After blocking with 1% BSA, the polyvinylidene fluoride membrane was incubated with the primary antibodies at 4°C overnight, followed by incubation with appropriate secondary antibody for 1 hour, and stained with enhanced chemiluminescence (ECL). The level of the targeted proteins was photographed and analyzed using a UVP gel analysis system (iBox Scientia 600; UVP, LLC., CA, USA).

Statistical Analysis

All data are presented as means ± standard deviation (SD). Independent-sample t-tests were used to compare means between two different groups. One-way analysis of

View Article Online
DOI: 10.1039/C9NR01255A

variance (ANOVA) was used to determine the level of significance with GraphPad Prism software and $P < 0.05$ was considered to be statistically significant.

Results

Characterization of Exo-cur

Cur treated RAW 264.7 cells were cultured and then Exo-cur was isolated from the culture supernatants of cells by ultracentrifugation. As shown in Fig. 2C, the markers of exosomes, Alix and CD63, were detected by western blot to confirm that Exo-cur was indeed isolated from the cells. Whereas Calnexin, expressed in endoplasmic reticulum, was not detected in exosomes. Furthermore, the expression of LFA-1 was evaluated on Exo-cur by western blot. It demonstrated that LFA-1 was highly expressed in Exo-cur, consistent with previous results [32, 33]. Therefore, Exo-cur inheriting LFA-1 can be used as a drug vehicle for targeting endothelial ICAM-1 and traversing the BBB. We also found that typical structures of Exo and Exo-cur accessed by TEM, DLS and AFM (Fig. 2A, 2B and 2D) showed that the Exo and Exo-cur presented normal morphological characteristics, with a diameter of approximately 100 nm. Size and zeta analysis revealed that the average sizes of Exo and Exo-cur were 110.3 ± 7.8 nm and 117.4 ± 10.5 nm, and the zeta potential were -4.5 mV and -4.9 mV. These characteristics indicated that the properties of exosomes were not affected by the modifications. According to the AFM images (Fig. 2D), the Exo and Exo-cur were round in shape and well dispersed. The average encapsulation efficiency and loading capacity of cur in Exo were 84.8% and 15.1%.

The in vitro release of cur from Exo was conducted by dialysis bag method and the

View Article Online
DOI: 10.1039/C9NR01255A

results (Fig. 2E) implied that free cur showed faster release rate and obtained a rapid cumulative release of 65.7% within 4 h, while the value was up to 86.7% within 24 h. On the contrary, Exo also controlled the slow and smooth release of cur and more than approximately 85.6% of total cur slowly leaked out from Exo into medium within 24 hours.

Fig. 2 Characterization and function study of Exo-cur: (A) Morphology of Exo and Exo-cur observed by TEM. (B) Particle size distribution measured by DLS. (C) Western blot analysis of Alix, CD63, Calnexin and LFA-1 from cur-primed RAW264.7, supernatant and Exo-cur. The supernatant obtained from the ultracentrifugation during exosome isolation was used as a negative control. (D) AFM images of Exo and Exo-cur. Upper graphs show peak force error images. Lower graphs present 3D height sensor images. Scale bar: 500 nm. (E) In vitro release profile of free-cur and Exo-cur in phosphate-buffered saline for 24 hours. Data are expressed as means ± SD (n=3).

Incorporation of cur into Exo can increase the solubility, stability, and bioavailability of cur

To determine whether the encapsulation of cur into Exo can increase cur's solubility, free-cur and Exo-cur at an identical amount of cur were added into an equal volume of PBS under continuous shaking for 30 mins. Especially, the solubility of Exo-cur was increased to 10 folds as compared to the free cur. Being consistent with the previous report [39], the solubility of crude cur was only 1.8 μg/mL, while the apparent solubility of exosomal cur was dramatically increased to 18.5 μg/mL (Fig. 3A). As cur is highly susceptible to hydrolysis or degradation in aqueous solution, the degradation rate of free cur was significantly higher than that of Exo-cur in PBS and

View Article Online
DOI: 10.1039/C9NR01255A

in plasma (Fig. 3B). The free cur degraded rapidly in the first 30 min in PBS and in plasma, and the total degradation exceeded 60% at 2 h. While, cur in Exo was protected from degradation and about 80% of total cur remained in PBS and plasma after the 120-minute incubation. All these results clearly depicted that compared with free cur, the solubility and stability of cur were evaluated to have been enhanced after being loaded into Exo.

To assess whether exosomal cur can increase bioavailability of cur, free cur, and Exo-cur were administered intravenously (i.v.) in SD rats for evaluating their pharmacokinetic profile. The time-dependent plasma concentration data of cur suspension and Exo-cur in rats shown in Fig. 3D demonstrated that the maximum plasma concentration (Cmax) of cur in free-cur treated group was peaked at 0.52 μg/mL after 5 min of administration, and then decreased rapidly. Cmax of cur in Exo-cur treated group was peaked at 2 h after administration and was significantly improved to 0.91 μg/mL. Compared with free-cur, Exo-cur also contributed to the higher bioavailability and slower metabolism rate by a substantial increase in plasma area under curve (AUC), a notably extended half-life ($t_{1/2}$) and a significant decrease in the total body clearance (CL) of cur.

Next, cur in different organs of SD rats was quantitatively analyzed by detecting fluorescence absorbance of cur to study free-cur and Exo-cur biodistributions (Fig. 3C). The results demonstrated that Exo-cur injection increased the accumulation of cur in the brain, liver and lung compared with those following free-cur treatment. The increase in brain targeting of Exo-cur compared to free-cur was greater than the

View Article Online
DOI: 10.1039/C9NR01255A

corresponding increase in the liver and lung. The accumulation of Exo-cur in the brain was 6.5 times higher than that of free-cur; while the accumulations of Exo-cur in the liver and lung were 2.5 times and 2.0 times higher than that of free-cur. It revealed that Exo could facilitate higher accumulation of cur in the brain.

Finally, histological differences were investigated to evaluate systemic toxicity of free-cur and Exo-cur in SD rats model. As indicated in Fig. 3E, compared with sham group (saline treatment), there was also no obvious histological difference of major organs in both free-cur and Exo-cur treated groups, which suggested that no significant toxicity was induced by free-cur and Exo-cur. These findings also suggested that Exo-cur potentially was a safe carrier for AD therapy.

Fig. 3 Encapsulation of cur into Exo can increase curcumin's solubility and stability in vitro. (A) Representative spectrographs of cur and exosomal cur in PBS, and the spectrographs were obtained using a fluorescence spectrophotometer (F-4600, Hitachi, Tokyo, Japan). (B) Exosomal cur is more stable than free curcumin. Cur and exosomal cur were added to 2 ml PBS and plasma to achieve a final concentration of 1.5 μg/mL and incubated in the dark in a 37 °C water bath. At 30, 60, 90 and 120 minutes, 100 μl of each sample was taken to determine the concentration of cur. The concentrations of cur or exosomal cur at the beginning were set as 1.00. The fold reduction of the concentration at each time point compared to the beginning was shown. Data are expressed as means ± SD (n=3). (C) Tissue distribution of cur in rats treated with Exo-cur or free-cur. Data are expressed as means ± SD (n=3), **P < 0.01. (D) The plasma concentration–time curve of cur and fitted PK parameters of cur in rat plasma after single i.v. administration of free cur and Exo-cur at the concentration of cur (0.4 mg/kg). Data are expressed as means ± SD (n=3), **P <

View Article Online
DOI: 10.1039/C9NR01255A

0.01. (E) H&E stainings of liver, lung and kidney tissue sections at 24 h after i.v. administering a single dose of 1 mL of saline and 1 mL of various cur formulations at 0.4 mg/kg. The scale bar is 200 μm and applies to all figure parts.

Exo-cur enhanced cellular uptake and BBB-crossing in Vitro

To evaluate whether the Exo-cur has acquired high enough targeting capability in vitro, the cellular uptake of free-cur and Exo-cur by the brain microvascular endothelial cell line (noted as hCMEC/D3), the main component of BBB, was intensively investigated. Confocal microscopic analysis of hCMEC/D3 (Fig. 4A) by co-culture with free-cur and Exo-cur revealed that when the cells were treated with free-cur, the green fluorescence intensity of the cells was weak, indicating that most of free-cur were not taken up by hCMEC/D3 and that only a small portion of free-cur were internalized into cells by endocytic process. Compared with the weak fluorescent dots observed in cells treated with free-cur**,** stronger and intense green fluorescence emitted by exosomal cur appeared in the cytoplasm owing to the specific binding between exosomes surface inherited LFA-1 and endothelial ICAM-1. To further clarify the internalization process of Exo-cur mediated by the interaction between LFA-1 and ICAM-1**,** Exo-cur was pre-incubated with ICAM-1 to block its LFA-1 and further treated with the cells to investigate the competitive cellular uptake mechanism of Exo-cur. The results showed that following the treatment of hCMEC/D3 with Exo-cur pre-treated with 2 mg/mL of ICAM-1 for blocking exosomes surface LFA-1, intracellular fluorescent intensity was significantly reduced and the Exo-cur uptake was significantly inhibited. This suggested that Exo-cur

View Article Online
DOI: 10.1039/C9NR01255A

selectively bound to cell surface ICAM-1 and accelerated the internalization of Exo-cur into cells. In addition, quantitative fluorescence intensity analysis of cur in hCMEC/D3 (Fig. 4A) by co-culture with free cur and Exo-cur also presents the highly consistent results with the confocal analysis.

To measure the BBB-crossing efficacy of free-cur and Exo-cur, the penetration rates of free-cur and Exo-cur across BBB were assessed by checking the fluorescence intensity of cur in the lower chamber using a microplate reader (Synery-2; BioTek Instruments), and they were calculated by determining the ratio of the fluorescence intensity of penetrated free-cur or Exo-cur in the lower chamber to that of the initially added free-cur or Exo-cur in the upper chamber. The results (Fig. 4B) showed that more than 60% of Exo-cur had penetrated across the BBB layer and detected on the lower chamber within 6 h. In comparison, only about 15% of free-cur was found under the same condition, indicating the significant targeting effect of Exo-cur compared with free-cur. To make sure whether the LFA-1 on Exo-cur had played a major role in mediating the BBB-crossing transcytosis with ICAM-1 or not, blocking assay was further employed. When ICAM-1 was used to pre-incubated with the Exo-cur to block the targeting interaction between LFA-1 and ICAM-1, the penetrating efficiency of Exo-cur was significantly reduced, as represented by the decreased penetration rates at about 40% within 6 h. These results clearly demonstrated the advantage of Exo-cur in transporting across the BBB by interaction between its inherited LFA-1 and endothelial ICAM-1, resulting in the enhanced intracephalic uptake and guaranteeing the following neuroprotection effect.

View Article Online
DOI: 10.1039/C9NR01255A

Fig. 4 Exo-cur enhanced cellular uptake and BBB-crossing in vitro. (A) The uptake of free-cur and Exo-cur in hCMEC/D3 for 6 hours. Data represent means ± SD (n = 3), * $P < 0.05$, # $P < 0.05$. The scale bar is 50 μm and applies to all figure parts. (B) Analysis of the penetration mechanism of cur and Exo-cur through hCMEC/D3 cells. Data represent means ± SD (n = 3), * $P < 0.05$, ** $P < 0.01$, # $P < 0.05$, ## $P < 0.01$.

Exo-cur enhanced accumulation of cur in brain in vivo

To monitor the distribution of free-cur and Exo-cur in brain, we prepared free-cur and Exo-cur administrating via intraperitoneal injection in C57BL/6 mice. In vivo imaging results shown in Fig. 5A that highly enhanced fluorescence of cur was observable in cerebral region in Exo-cur treated group in contrast with weakening fluorescent intensity fluorescence of cur in free-cur treated group at 6h and 24 h after treatment. To determine whether free-cur and Exo-cur can be target-delivered in hippocampus, we observed the distribution of cur in hippocampus in C57BL/6 mice brain tissue slices. It was found in Fig. 5B that the green fluorescent intensity emitted by cur was stronger in hippocampus in Exo-cur treated group compared with free-cur treated group. To further determine the intracellular distribution of free-cur and Exo-cur in the brain tissue, brain slices were obtained and stained with neuron cell marker NeuN. It demonstrated that the fluorescence of Exo-cur was intense and well co-localized with NeuN-positive neuron cells in hippocampus, showing in Fig. 5C, suggesting that Exo-cur had been delivered into neuron cells in hippocampus of the brain. These data indicated that Exo-cur enhanced accumulation of cur in hippocampus of brain in vivo, which contributed to neuroprotective effects.

View Article Online
DOI: 10.1039/C9NR01255A

Fig. 5 The accumulation of cur in hippocampus of brain tissue in C57BL/6 mice model. (A) Representative fluorescence images (overlaid with photograph) of C57BL/6 mice brains which received the i.p. administration of free-cur and Exo-cur. Brains were dissected 6 h and 24 h after administration. (B) Representative fluorescent images of free-cur and Exo-cur at hippocampus from C57BL/6 mice receiving after 6 h of i.p. administration of free-cur and Exo-cur. The scale bar is 25 μm and applies to all figure parts. (C) Co-location of free-cur and Exo-cur (green) with neuron cells in hippocampus of brain tissue. Neuron cells were stained with anti-NeuN (red). The scale bar is 50 μm and applies to all figure parts.

Exo-cur induced Neuroprotection in OA-induced AD mice model

As the survival of neuron in the hippocampus is closely correlated with good outcomes for AD therapy, we finally evaluated whether Exo-cur treatment could decrease neuron injury in hippocampus. Live neuron cells in the hippocampus was observed and counted by staining them with NeuN. The results (Fig. 6) revealed that after OA was used to induce AD, neuronal cells in hippocampus were seriously damaged and the numbers of NeuN-positive cells in hippocampal CA1 region, CA3 region and DG region in OA group were significantly reduced in contrast with sham group ($P<0.01$). Interestingly, Exo-cur group had more NeuN-positive cells in hippocampal CA1 region, CA3 region and DG region than that of OA group and OA+cur group ($P<0.01$). The result demonstrated that Exo-cur treatment could effectively reduce OA induced neuronal injury.

Fig. 6 Representative immunofluorescence staining for Neuron positive cells in hippocampal CA1 region, CA3 region and DG region after 7 days of daily peritoneal injection of free-cur and

View Article Online
DOI: 10.1039/C9NR01255A

Exo-cur. NeuN antibodies were used to stain neurons in the hippocampus. DAPI (blue) was used as a nuclear marker. The scale bar is 100 μm and applies to all figure parts. Data are expressed as means ± SD (n=3). ** P < 0.01,## indicating P<0.01, compared OA+Exo-cur group with OA group.

Exo-cur attenuates OA-induced cognitive decline

To evaluate the therapeutic efficiency of our Exo-cur in vivo, after establishment of OA induced AD model mice for 5 days, saline, Exo, free cur and Exo-cur were administered via a single peritoneal injection daily for consecutive 7 days. The animal experimental design was depicted in Fig. 7A. The in vivo therapeutic efficiency was examined by Morris water maze test at 7 days post treatment. The Morris water maze task is a popular and well-validated test for spatial learning, and is one of the most-used behavioral tests in neuroscience research with mouse models. It demonstrated that from 1 day to 5 days, escape latency time in OA treated group is significantly longer than that in sham group and there was significant difference (P <0.01) between sham group and OA treated group (Fig. 7B). Moreover, in the probe trial, after the platform was removed, the OA treated mice induced the lower target quadrant occupancy and numbers of crossing compared with that in sham group (Fig. 7C, D, E), indicating that OA administration impaired memory and spatial learning ability of the mice. We also observed that compared with OA induced AD mice model, Exo-cur treated mice showed the shorter escape latencies and exhibited spatially oriented swimming behavior, they spent longer time in the target quadrant and increased the numbers of crossing (Fig. 7C, D, E), indicating that administration

View Article Online
DOI: 10.1039/C9NR01255A

of Exo-cur remarkably improved memory and spatial learning ability of the mice in OA induced AD mice model. On the contrary, when free-cur was administrated, there was no notable difference in escape latencies or target quadrant occupancy compared with the OA group ($P > 0.05$; Fig. 7B, D). Therefore, it is considered that Exo-cur can significantly rescue memory disorder in the OA induced AD mice model by effectively reducing the escape latency of model mice and enhancing the percent of occupancy in target quadrant and virtual-platform crossing times. Moreover, Exo-cur can be considered to be more effective than free cur in ameliorating learning and memory impairments in AD model mice.

Fig. 7 Exo-cur ameliorates the cognitive deficiency in OA treated mice. (A) Experimental design for the animal study. (B) Escape latencies.analysis. Data are expressed as means ± SD (n=3). * $P < 0.05$, ** $P < 0.01$,## indicating $P<0.01$, compared OA+Exo-cur group with OA group. (C) The platform crossing number in the spatial probe test. Data are expressed as means ± SD (n=3). * $P <$ 0.05, ** $P < 0.01$,## indicating $P<0.01$, compared OA+Exo-cur group with OA group. (D) Relative time percentage spent on the target quadrant in a probe trial. Data are expressed as means ± SD (n=3). * $P < 0.05$, ** $P < 0.01$,## indicating $P<0.01$, compared OA+Exo-cur group with OA group. (E) Representative path tracings of different groups.

Exo-cur reverses the cognitive dysfunction of AD mice by reducing OA-induced cell apoptosis

It was well known that the death of neuron cells in hippocampus also resulted in the cognitive dysfunction of AD mice. Here we investigated the role of Exo-cur on reversing OA-mediated cell death in hippocampus by WB. The results (Fig. 8B)

View Article Online
DOI: 10.1039/C9NR01255A

showed that compared to the sham group, OA group showed the highest expression of bax and cleaved caspase-3, indicating that OA aggravated the neuronal damage in hippocampus and cell apoptosis effects were significantly enhanced through the injection of OA in hippocampus. However, compared with the OA group, expressions of bax and cleaved caspase-3, were significantly decreased by administration of Exo-cur. Meanwhile, as compared with cur, Exo-cur showed the better anti-apoptosis effects by inducing the lower expressions of bax and cleaved caspase-3 ($P < 0.05$). These results revealed that the Exo-cur may significantly reduce OA induced cytotoxicity of neuron cells, thus indicating its significant neuroprotective effects in AD mice by increasing neuron survival.

Exo-cur rescues the phosphorylation of Tau protein by OA in vivo

To test the protective effect of Exo-cur on the over-phosphorylation of Tau protein induced by OA, we examined the levels of p-Tau (Ser396) using a western blot assay. OA group showed a higher expression level of p-Tau (Ser396) than the sham group ($P < 0.01$), which indicated that OA administration induced the Tau hyperphosphorylation. However, Exo-cur treatment induced the lower Tau phosphorylation than OA group. Furthermore, as compared with cur, Exo-cur displayed the stronger inhibition of OA-induced increase in p-Tau (Ser396) ($P < 0.01$). These experiments indicated that Exo-cur inhibited OA-induced phosphorylation of Tau protein. However, the cellular signal pathway is needed to be further investigated.

Exo-cur activates AKT and inhibits tau phosphorylation through the AKT /GSK-3β pathway in vivo

View Article Online
DOI: 10.1039/C9NR01255A

To further study how Exo-cur regulated Tau phosphorylation, western blot assay was performed to examine the associated proteins. It was known that GSK-3β participated in the phosphorylation of Tau protein. When GSK-3β was activated, it was dephosphorylated at residues Ser9 and induced phosphorylation of Tau protein. Compared with the sham group, the level of phosphorylation of GSK-3β at Ser9 is significantly reduced in the OA group ($P < 0.01$). This implied that OA resulted in activation of GSK-3β. In Exo-cur group, however, phosphorylation of GSK-3β at Ser9 is increased significantly compared with OA group ($P < 0.01$) (Fig. 8B). This implied that Exo-cur inhibited OA-induced activation of GSK-3β protein. AKT was a potential upstream regulator of GSK-3β and the activated AKT inhibited the activation of GSK-3β by promoting phosphorylation of GSK-3β at Ser9. We also investigated the role of AKT in OA-induced phosphorylation of Tau. The results showed that compared with the sham group, the level of phosphorylation of AKT is significantly reduced in the OA group ($P < 0.01$). This implied that OA resulted in deactivation of AKT. In Exo-cur group, however, phosphorylation of AKT is increased significantly compared with OA group ($P < 0.01$) (Fig. 8). Meanwhile, as compared with cur, the levels of phosphorylation of GSK-3β at Ser9 and AKT were significantly up-regulated in Exo-cur group ($P < 0.05$). This result indicated that AKT mediated the protection of cur against OA-induced activation of GSK-3β and Tau phosphorylation.

Fig. 8 In vivo therapeutic mechanism of Exo-cur in OA induced AD mice model. (A) A proposed model illustrating the mechanism underlying the efficiency of Exo-cur in the amelioration of

View Article Online
DOI: 10.1039/C9NR01255A

cognitive impairment in AD. Exo-cur rescued neuronal cells from apoptosis by regulating pro-apoptotic proteins. Moreover, Exo-cur also inhibited Tau phosphorylation by activating AKT/GSK-3β pathway. (B) Western blot and quantification results of p-AKT, Tau, p-Ser396 Tau, p-Ser9 GSK-3β, Bax and C-Caspase 3 in hippocampus of OA induced AD mice after treatment with free cur and Exo-cur. Data are expressed as means ± SD (n=3). * $P < 0.05$, ** $P < 0.01$,## indicating $P<0.01$, compared OA+Exo-cur group with OA group.

Naïve Exo attenuates OA-induced cognitive decline by regulating microglia and neuron cells

We had confirmed that Exo-cur potently ameliorated cognitive function in AD mice by inhibiting phosphorylation of Tau protein through the AKT/GSK-3β pathway. However, role of naïve Exo secreted by macrophage in the pathogenesis of AD was still unknown. Therefore, we made a primary investigation on the effect of naïve Exo on attenuating OA-induced learning and memory deficits in Tau-phosphorylated AD-like mouse model and explored its neuroprotective effects. The results (Fig. 9A) demonstrated that escape latency time in OA+Exo treated group is significantly shorter than that in OA treated group ($P <0.01$). In probe trials, OA+Exo treated mice showed an enhanced percentage of occupancy in target quadrant and virtual-platform crossing times compared with the OA group ($P < 0.05$). However, relative to OA+Exo-cur treated group, OA+Exo treated group resulted in the longer escape latency time, lower percentage of occupancy in target quadrant and virtual-platform crossing times. It confirmed that although improvement of the cognitive disorder by Exo was limited and lower than that of Exo-cur group, Exo

View Article Online
DOI: 10.1039/C9NR01255A

administration still played the synergistic role on reducing OA induced impaired memory and improving spatial learning ability in AD mice. As Exo secreted by macrophage contained elevated levels of cytokines and miRNAs and regulated inflammation by transiting the early pro-inflammatory gene transcription to anti-inflammatory gene transcription [40], it was highly associated with the regulation of inflammation. It was also reported that generation of Tau protein phosphorylation could induce neuroinflammation by activating microglia, the major immune cells in the central nervous system, the activated microglia then induced neuronal injury due to the secretion of various proinflammatory molecules [41-42]. Therefore, we supposed that since Exo could be highly associated with the regulation of inflammation, its alleviation on OA-induced memory impairments could probably attribute to reduced neuroinflammation by preventing the OA-induced microglia over activation and reducing OA-triggered apoptotic response in the hippocampus. Our results demonstrated that when the intracellular distribution of Exo in microglia of brain from hippocampus was detected by labeling Exo with DiI (red) and staining brain slices with microgial cell marker Iba1 (green), the red fluorescence of Exo was intense and well co-localized with Iba1-positive microglia in brain, showing in Fig. 9B, suggesting that Exo had been internalized into microglia in the brain. As shown in Fig. 9C, typical images in hippocampus showed that OA group had the more number and density of the Iba-1 positive cells compared to sham group, indicating that OA induced the activation of microglia, leading to its neurotoxicity by accelerating the release of neurotoxic pro-inflammatory factors by microglia. Compared with OA

View Article Online
DOI: 10.1039/C9NR01255A

group, Exo significantly decreased the number and density of the Iba-1-positive cells. Western blot results and immunofluorescence staining (Fig. 9D and 9E) also confirmed that Iba-1 levels were elevated in the hippocampus of OA induced AD model mice. Exo treatment significantly decreased Iba-1 expression in the hippocampus of brain tissues in AD model mice. Furthermore, Exo did decrease phosphorylation of Tau protein at Ser396 as compared with OA group ($P<0.05$). The results (Fig. 9F) revealed that Exo group has more NeuN-positive cells in hippocampal CA1 region, CA3 region and DG region than that of OA group, indicating that Exo treatment could effectively reduce OA induced neuronal injury by preventing OA-triggered apoptotic response in the hippocampus. The above data suggested that Exo inhibited abnormal activation of microglia in vivo and reduced OA induced apoptosis of neuronal cells, thus indicating its neuroprotective effects.

Fig. 9 Naïve Ex attenuates OA-induced cognitive decline in AD mice by relieving over-activation of microglia and reducing OA induced apoptosis of neuronal cells. (A) Hidden platform learning histograms. Subsequent histograms represent average of all daily trials. Data are expressed as means ± SD (n=3). *$p < 0.05$, **$p < 0.01$, ## indicating $P<0.01$, compared OA+Exo-cur group with OA group.(B) Co-location of DiI-labeled Exo with microglia cells in hippocampus of OA induced AD mice. Microglia was stained with anti-Iba1 (green). The scale bar is 50 μm and applies to all figure parts. (C) Brain tissues were fixed and stained with Iba-1 antibody, then imaged by immunofluorescence confocal microscopy (red). Nuclei were stained with DAPI (blue). Representative image demonstrating the morphology of microglia in hippocampus. The scale bar is 50 μm and applies to all figure parts. (D) Western blot results of Iba-1 and p-Ser396 Tau in

View Article Online
DOI: 10.1039/C9NR01255A

hippocampus of OA induced AD mice after treatment with Exo. Data are expressed as means ± SD (n=3). *p < 0.05, **p < 0.01. (E) Representative immunofluorescence staining of p-Ser396 Tau in hippocampus of OA induced AD mice after treatment with Exo. DAPI (blue) was used as a nuclear marker. The scale bar is 100 μm and applies to all figure parts. (F) Representative immunofluorescence staining for Neuron positive cells in hippocampal CA1 region, CA3 region and DG region after peritoneal injection of Exo. NeuN antibodies were used to stain neurons in the hippocampus. DAPI (blue) was used as a nuclear marker. The scale bar is 100 μm and applies to all figure parts. Data are expressed as means ± SD (n=3). **p < 0.01.

Discussion

At present, Tau protein phosphorylation is recognized as one of the neuropathological mechanisms of AD. In elderly patients with dementia, the level of Tau protein is 300% higher than normal elderly, and the hyperphosphorylated Tau protein plays a major role in the pathogenesis of AD [43]. Tau protein is regarded as a microtubule-associated protein and its phosphorylation is regulated by protein kinase and protein phosphatase. Okadaic acid (OA), a specific inhibitor of protein phosphatase PP2A, can hyperphosphorize Tau protein in neuronal cells [34]. It was reported that over-phosphorylated Tau protein decreased binding to microtubules, and the stability of microtubules was reduced to damage the homeostasis of the nervous system. Finally, phosphorylated Tau protein was accumulated to form double-stranded filaments, resulting in the formation of neurofibrillary tangles, which in turn destroys the normal function of neurons and ultimately leads to AD. Modern pharmacological studies have shown that cur has neuroprotective effects and

View Article Online
DOI: 10.1039/C9NR01255A

improves cognitive function in AD treatment. A large number of studies have shown that cur decreases phosphorylation of Tau by down-regulating Caveolin-1/GSK-3β in N2a/APP695swe cells and APP/PS1 double transgenic Alzheimer's Disease mice [31]. Furthermore, cur attenuates amyloid-b-induced Tau hyperphosphorylation in human neuroblastoma SH-SY5Y cells involving PTEN/Akt/GSK-3β signaling pathway [32]. However, cur's poor bioavailability resulted from a very low aqueous solubility is a major disadvantage that limited its wide use as a therapeutic agent [44]. Thus several types of cur loaded nanoformulations, such as liposomes, polymeric nanoparticles, cyclodextrins , solid dispersions and micelles were developed to achieve increased bioavailability and were widely applied into clinical researches [45-46]. Recent studies have indicated the importance of exosome therapy for AD [47-48]. Exosome is a promising tool to encapsulate drugs and target specific cells across different biological barriers, and further facilitates intercellular communication. In this study, we choose exosomes derived from curcumin-treated (primed) macrophage since incorporation of curcumin into exosomes can increase the solubility, stability, and bioavailability of curcumin. Our current study provides the direct evidence that incorporation of cur into exosomes increased solubility and stability of cur, and resulted in drug sustained release. Importantly, the naïve macrophage exosome can utilize the interaction between LFA-1 and ICAM-1 to interact with brain microvessel endothelial cells comprising the BBB and promote the penetration of cur cross the BBB into the brain. Notably, Exo-cur potently ameliorated cognitive function in AD mice by inhibiting OA induced phosphorylation of Tau protein. Although the

View Article Online
DOI: 10.1039/C9NR01255A

mechanism for inhibiting hyperphosphorylation of Tau protein is currently unclear, AKT/GSK-3β cellular pathway was generally regarded as an important signaling pathway for neuronal survival and one of the most important signaling pathways regulating the phosphorylation of Tau protein. As an important upstream regulator of GSK-3β, activated AKT inhibited the activation of GSK-3β by promoting phosphorylation of GSK-3β at Ser9 and further reduced phosphorylation of Tau protein. In this study, we found that in OA induced AD mice model, Exo-cur activated AKT and inhibited GSK-3β, finally reducing phosphorylation of Tau protein. It suggested that Exo-cur reduced OA-induced Tau protein phosphorylation through the AKT/GSK-3β signaling pathway. In addition, we further explored whether naïve Exo can improve cognitive function in OA induced AD mice model. The results demonstrated that Exo played synergistic neuroprotective effects by inhibiting abnormal activation of microglia in vivo and reducing OA induced apoptosis of neuronal cells. Taken together, Exo-cur enhanced BBB-crossing of cur via receptor-mediated transcytosis and potently ameliorated cognitive function in AD mice by inhibiting phosphorylation of Tau protein through the AKT/GSK-3β pathway. These data suggested that Exo-cur is a potential treatment not only for Alzheimer's disease, but also for other Tau hyperphosphorylation associated neurodegenerative diseases.

Conclusions

Compared with free cur, the incorporation of cur into Exo enhanced the solubility, stability, and bioavailability of cur. Owing to the interaction between exosomes

View Article Online
DOI: 10.1039/C9NR01255A

inherited LFA-1 and endothelial ICAM-1, Exo penetrated the BBB to the brain and a large amount of exosomal cur was distributed in hippocampus. Our study also showed that Exo-cur inhibited Tau phosphorylation through the AKT/GSK-3β pathway, contributing to the effective amelioration of learning and memory deficiencies in OA-induced AD mice. These findings provided further evidence for the potential clinical benefit of Exo-cur for AD treatment.

Disclosure statement

The authors report no conflicts of interest in this work.

Acknowledgement

This work was supported by grants from National Natural Science Foundation of China (81501017, 81502484), Natural Science Foundation of Liaoning Province (201602337), Scientific Research Project of Liaoning Provincial Department of Education (JYTQN201719). We thank the support of the above funds.

References

1. Prince M., Comas-Herrera A., Knapp M., Guerchet M., Karagiannidou M. In Proceedings of the World Alzheimer Report at Alzheimer's Disease International: London, UK, September, 2016.
2. Beyreuther K. Proc Natl. Acad. Sci. USA. 1985; 82:4245-4249.
3. Holtzman D.M., Morris J.C., Goate A.M. Sci. Transl. Med. 2011; 3:77sr1.
4. Hardy J., Selkoe D.J. Science. 2002; 297:353-356.
5. Doody R. S., Raman R., Farlow M., Iwatsubo T., Vellas B., Joffe S., Kieburtz K., He F., Sun X., Thomas R. G., Aisen P. S., Siemers E., Sethuraman G., Mohs R. N. Engl. J. Med. 2013; 369:341-350.
6. Salloway S., Sperling R., Fox N. C., Blennow K., Klunk W., Raskind M., Sabbagh M.,

Honig L. S., Porsteinsson A. P., Ferris S., Reichert M., Ketter N., Nejadnik B., Guenzler V. Miloslavsky M., Wang D., Lu Y., Lull J., Tudor I. C., Liu E., et al. N. Engl. J. Med. 2014; 370:322-333.

7. Doody R. S., Thomas R. G., Farlow M., Iwatsubo T., Vellas B., Joffe S., Kieburtz K., Raman R., Sun X., Aisen P. S., Siemers E., Liu-Seifert H., Mohs R. N. Engl. J. Med. 2014; 370:311-321.
8. Whittington R. A., Bretteville A., Dickler M. F., Planel E. Prog. Neuropsychopharmacol Biol. Psychiatry. 2013; 47:147-155.
9. Liu R., Zhou X. W., Tanila H., Bjorkdahl C., Wang J. Z., Guan Z. Z., Cao Y., Gustafsson J. A., Winblad B., Pei J. J. J. Cell Mol. Med. 2008; 12:241-257.
10. Ye S., Wang T. T., Cai B., Wang Y., Li J., Zhan J. X., Shen G. M. Neural. Regen. Res. 2017; 12:1479-1484.
11. Lu Y., He H. J., Zhou J., Miao J. Y., Lu J., He Y. G., Pan R., Wei Y., Liu Y., He R. Q. J Alzheimers Dis. 2013; 37:551-563.
12. Metaxas A., Kempf S. J. Neural. Regen. Res. 2016; 11:1579-1581.
13. Iqbal K., Gong C. X., Liu F. Expert Opin. Ther. Targets. 2014; 18:307-318.
14. Re F., Gregori M., Masserini M. Nanomed. Nanotechnol. Biol. Med. 2012; 73: 45–51.
15. Elias D., Blot F., Otmany A. El., Antoun S., Lasser P., Boige V., Rougier P., Ducreux M. Cancer. 2001; 92:71–76.
16. Pardridge W.M. Int. Congr. Ser. 2005; 1277:49–62.
17. Maussang D., Rip J., van Kregten J., van den Heuvel A., van der Pol S., van der Boom B., Reijerkerk A., Chen L., de Boer M., Gaillard P., de Vries H. Drug Discov. Today Technol. 2016; 20:59–69.
18. Zhang B., Wang M., Gong A., Zhang X., Wu X., Zhu Y., Shi H., Wu L., Zhu W., Qian H., Xu W. Stem. cells. 2015; 33:2158-2168.
19. EL Andaloussi S., Mäger I., Breakefield X. O., Wood M. J. Nat Rev Drug Discov. 2013; 12:347-357.
20. Johnsen K. B., Gudbergsson J. M., Skov M. N., Pilgaard L., Moos T., Duroux M. Biochim Biophys Acta. 2014; 1846:75-87.

21. Aqil F., Munagala R., Jeyabalan J., Agrawal A. K., Gupta R. AAPS J. 2017; 19:1691-1702.

22. Li H., Yang C., Shi Y., Zhao L. J Nanobiotechnology. 2018; 16:103.

23. Batrakova E. V., Kim M. S. J. Control Release. 2015; 219:396-405.

24. Qu M., Lin Q., Huang L., Fu Y., Wang L., He S., Fu Y., Yang S., Zhang Z., Zhang L., Sun X. J Control Release. 2018; 287:156-166.

25. Kim M. S., Haney M. J., Zhao Y., Yuan D., Deygen I., Klyachko N. L., Kabanov A.V., Batrakova E. V. Nanomedicine. 2018; 14:195-204.

26. Pinheiro A., Silva A. M., Teixeira J. H., Gonçalves R. M., Almeida M.I., Barbosa M. A., Santos S. G. Control Release. 2018; 289:56-69

27. Liao W., Du Y., Zhang C., Pan F., Yao Y., Zhang T., Peng Q. Acta Biomater. 2019;86:1-14.

28. van Niel G., D'Angelo G., Raposo G. Nat Rev Mol Cell Biol. 2018;19:213-228.

29. Okuda M., Hijikuro I., Fujita Y., Teruya T., Kawakami H., Takahashi T., Sugimoto H. Bioorg Med Chem Lett. 2016; 26:5024-5028.

30. Sun J., Zhang X., Wang C., Teng Z., Li Y. Am. J. Chin. Med. 2017; 45:1667-1682.

31. Huang H. C., Tang D., Xu K., Jiang Z. F. J. Recept. Signal Transduct. Res. 2014; 34:26-37.

32. Muller W. A. Vet. Pathol. 2013; 50:7-22.

33. Yuan D., Zhao Y., Banks W. A., Bullock K. M., Haney M., Batrakova E., Kabanov A.V. Biomaterials. 2017; 142:1-12.

34. Xu A. H., Yang Y., Sun Y. X., Zhang C. D. Neural. Regen Res. 2018; 13:2173-2181.

35. Cakir M., Duzova H., Tekin S., Taslıdere E., Kaya GB., Cigremis Y., Ozgocer T., Yologlu S. Life Sci. 2017;176:10-20.

36. Çakır M., Tekin S., Doğanyiğit Z., Erden Y., Soytürk M., Çiğremiş Y., Sandal S. Life Sci. 2019; 217:25-33.

37. Broetto N., Hansen F., Brolese G., Batassini C., Lirio F., Galland F., Dos Santos J. P., Dutra M.F., Gonçalves C. A. Brain Res. Bull. 2016; 124:136-143.

38. Wang L. L., He D. D., Wang S. X., Dai Y. H., Ju J. M., Zhao C. L. Drug Dev. Ind. Pharm. 2018; 44:563-569.

39. Kurien B. T., Singh A., Matsumoto H., Scofield R. H. Assay Drug Dev. Technol. 2007; 5:567-576.

40. McDonald M. K., Tian Y., Qureshi R. A., Gormley M., Ertel A., Gao R., Aradillas Lopez E., Alexander G. M., Sacan A., Fortina P., Ajit S. K. Pain. 2014; 155:1527-1539.

41. Heneka M. T., Carson M. J., El Khoury J., Landreth G. E., Brosseron F., Feinstein D. L., Jacobs A. H., Wyss-Coray T., Vitorica J., Ransohoff R. M., Herrup K., Frautschy S. A., Finsen B., Brown G. C., Verkhratsky A., Yamanaka K., Koistinaho J., Latz E., Halle A., Petzold G. C., Town T., etal. Lancet Neurol. 2015; 14:388-405.

42. Chan E. W. L., Krishnansamy S., Wong C., Gan S. Y. Neurotoxicology. 2018; 70:91-98

43. Banzhaf-Strathmann J., Benito E., May S., Arzberger T., Tahirovic S., Kretzschmar H., Fischer A., Edbauer D. EMBO J. 2014; 33:1667-1680.

44. Kurien B. T., Singh A., Matsumoto H., Scofield R. H. Assay Drug Dev. Technol. 2007; 5:567-576.

45. Karewicz A., Bielska D., Gzyl-Malcher B., Kepczynski M., Lach R., Nowakowska M. Colloids Surf. B Biointerfaces. 2011; 88:231-239.

46. Escalona-Rayo O., Fuentes-Vázquez P., Leyva-Gómez G., Cisneros B., Villalobos R., Magaña J. J., Quintanar-Guerrero D. Drug Dev. Ind. Pharm. 2017; 43:871-888.

47. Reza-Zaldivar E. E., Hernández-Sapiéns M. A., Minjarez B., Gutiérrez-Mercado Y. K., Márquez-Aguirre A. L., Canales-Aguirre A. A. Front Cell Neurosci. 2018; 12:317.

48. Iranifar E., Seresht B. M., Momeni F., Fadaei E., Mehr M. H., Ebrahimi Z., Rahmati M., Kharazinejad E., Mirzaei H. J. Cell Physiol. 2019; 234:2296-2305.

View Article Online
DOI: 10.1039/C9NR01255A

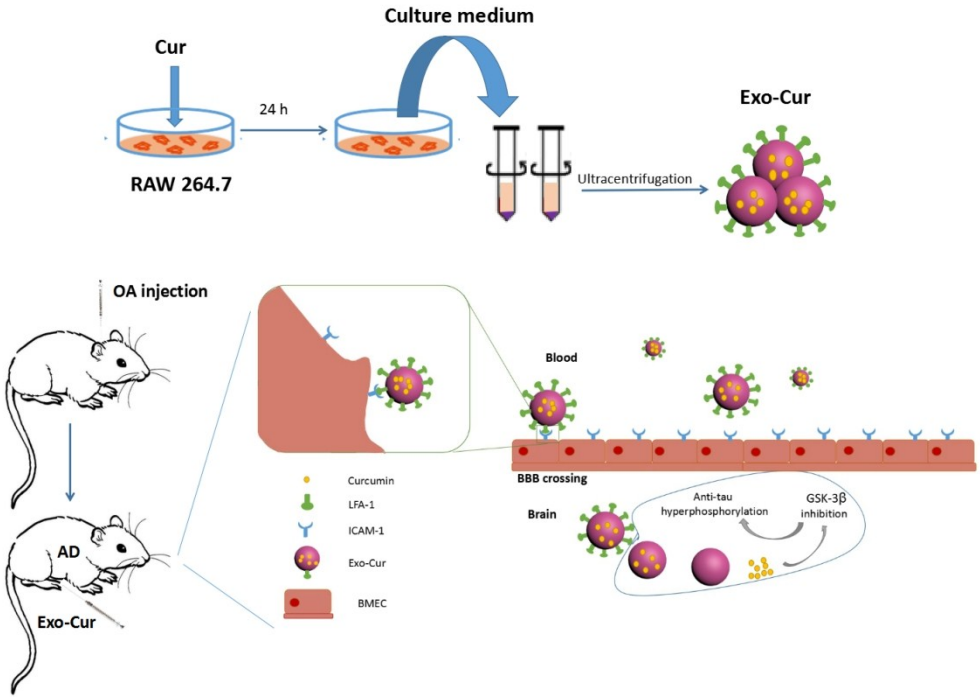

Fig. 1 The primary hypothesis of this study. Exosomes derived from curcumin-treated (primed) cells (Exo-cur) can better relieve the symptoms of AD by inhibiting phosphorylation of Tau protein through AKT/GSK-3β pathway. Exo-cur secreted by cur treated RAW 264.7 was collected and purified by ultracentrifugation. The safe and effective delivery of cur across the blood–brain barrier (BBB) due to the interaction between Exo inherited LFA-1 and endothelial ICAM-1 was demonstrated in vivo and in vitro. Furthermore, Exo-cur inhibited OA-induced phosphorylation of Tau and ameliorated cognitive function in AD mice. It demonstrated that the novel Exo-cur had a target treatment capability for AD and can traverse the BBB, indicating the potential for the effective treatment of AD.

506x353mm (72 x 72 DPI)

View Article Online
DOI: 10.1039/C9NR01255A

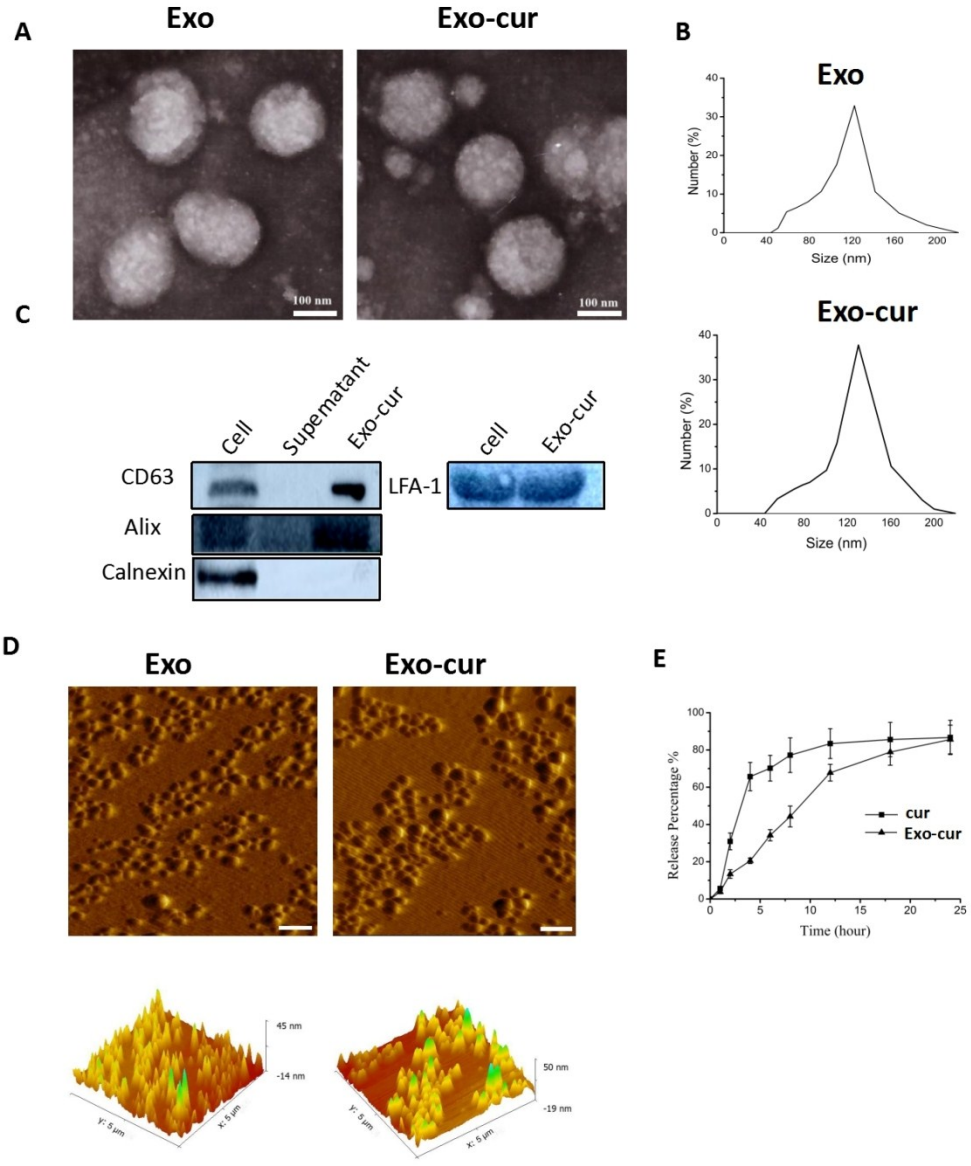

Fig. 2 Characterization and function study of Exo-cur: (A) Morphology of Exo and Exo-cur observed by TEM. (B) Particle size distribution measured by DLS. (C) Western blot analysis of Alix, CD63, Calnexin and LFA-1 from cur-primed RAW264.7, supernatant and Exo-cur. The supernatant obtained from the ultracentrifugation during exosome isolation was used as a negative control. (D) AFM images of Exo and Exo-cur. Upper graphs show peak force error images. Lower graphs present 3D height sensor images. Scale bar: 500 nm. (E) In vitro release profile of free-cur and Exo-cur in phosphate-buffered saline for 24 hours. Data are expressed as means ± SD (n=3).

View Article Online
DOI: 10.1039/C9NR01255A

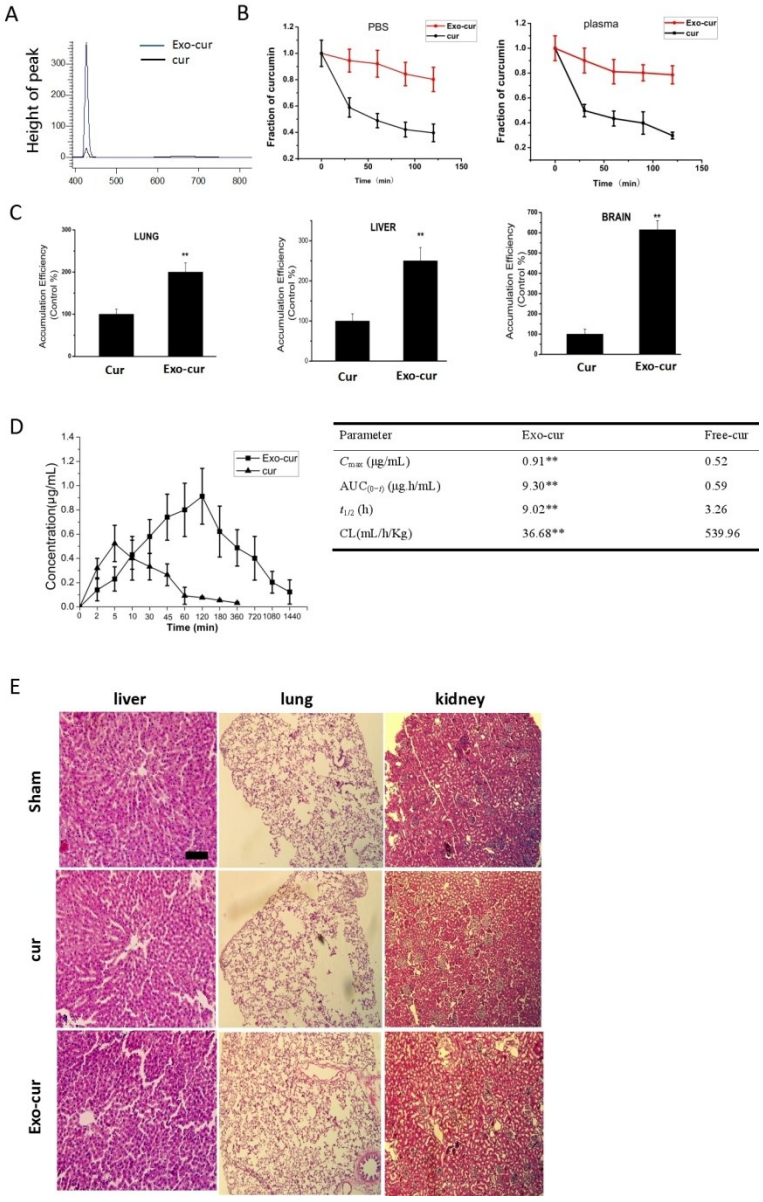

Parameter	Exo-cur	Free-cur
C_{max} (μg/mL)	0.91**	0.52
$AUC_{(0-t)}$ (μg.h/mL)	9.30**	0.59
$t_{1/2}$ (h)	9.02**	3.26
CL(mL/h/Kg)	36.68**	539.96

Fig. 3 Encapsulation of cur into Exo can increase curcumin's solubility and stability in vitro. (A) Representative spectrographs of cur and exosomal cur in PBS, and the spectrographs were obtained using a fluorescence spectrophotometer (F-4600, Hitachi, Tokyo, Japan). (B) Exosomal cur is more stable than free curcumin. Cur and exosomal cur were added to 2 ml PBS and plasma to achieve a final concentration of 1.5 μg/mL and incubated in the dark in a 37 °C water bath. At 30, 60, 90 and 120 minutes, 100 μl of each sample was taken to determine the concentration of cur. The concentrations of cur or exosomal cur at the beginning were set as 1.00. The fold reduction of the concentration at each time point compared to the beginning was shown. Data are expressed as means ± SD (n=3). (C) Tissue distribution of cur in rats treated with Exo-cur or free-cur. Data are expressed as means ± SD (n=3), **P < 0.01. (D) The plasma concentration–time curve of cur and fitted PK parameters of cur in rat plasma after single i.v. administration of free cur and Exo-cur at the concentration of cur (0.4 mg/kg). Data are expressed as means ± SD (n=3), **P < 0.01. (E) H&E stainings of liver, lung and kidney tissue sections at 24 h after i.v. administering a single dose of 1 mL of saline and 1 mL of various cur formulations at 0.4 mg/kg. The scale bar is 200 μm and applies to all figure parts.

View Article Online
DOI: 10.1039/C9NR01255A

480x757mm (72 x 72 DPI)

View Article Online
DOI: 10.1039/C9NR01255A

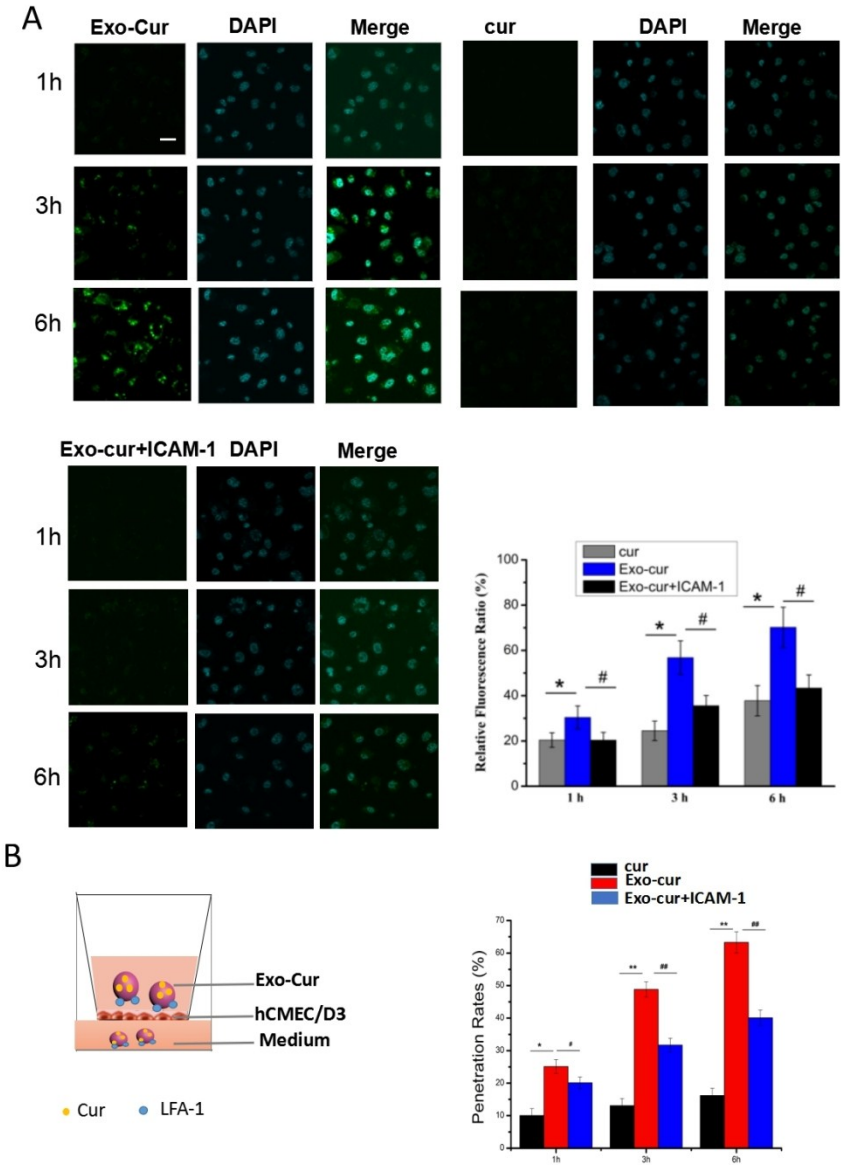

Fig. 4 Exo-cur enhanced cellular uptake and BBB-crossing in vitro. (A) The uptake of free-cur and Exo-cur in hCMEC/D3 for 6 hours. Data represent means ± SD (n = 3), * $P < 0.05$, # $P < 0.05$. The scale bar is 50 μm and applies to all figure parts. (B) Analysis of the penetration mechanism of cur and Exo-cur through hCMEC/D3 cells. Data represent means ± SD (n = 3), * $P < 0.05$, ** $P < 0.01$, # $P < 0.05$, ## $P < 0.01$.

View Article Online
DOI: 10.1039/C9NR01255A

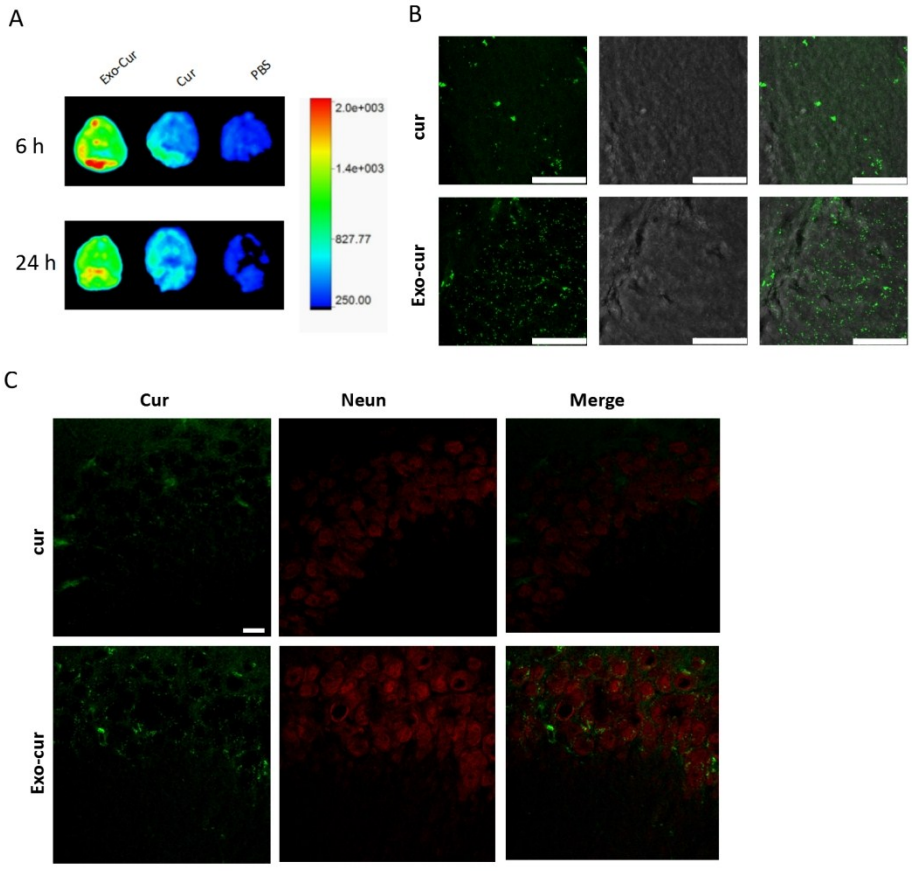

Fig. 5 The accumulation of cur in hippocampus of brain tissue in C57BL/6 mice model. (A) Representative fluorescence images (overlaid with photograph) of C57BL/6 mice brains which received the i.p. administration of free-cur and Exo-cur. Brains were dissected 6 h and 24 h after administration. (B) Representative fluorescent images of free-cur and Exo-cur at hippocampus from C57BL/6 mice receiving after 6 h of i.p. administration of free-cur and Exo-cur. The scale bar is 25 μm and applies to all figure parts. (C) Co-location of free-cur and Exo-cur (green) with neuron cells in hippocampus of brain tissue. Neuron cells were stained with anti-NeuN (red). The scale bar is 50 μm and applies to all figure parts.

View Article Online
DOI: 10.1039/C9NR01255A

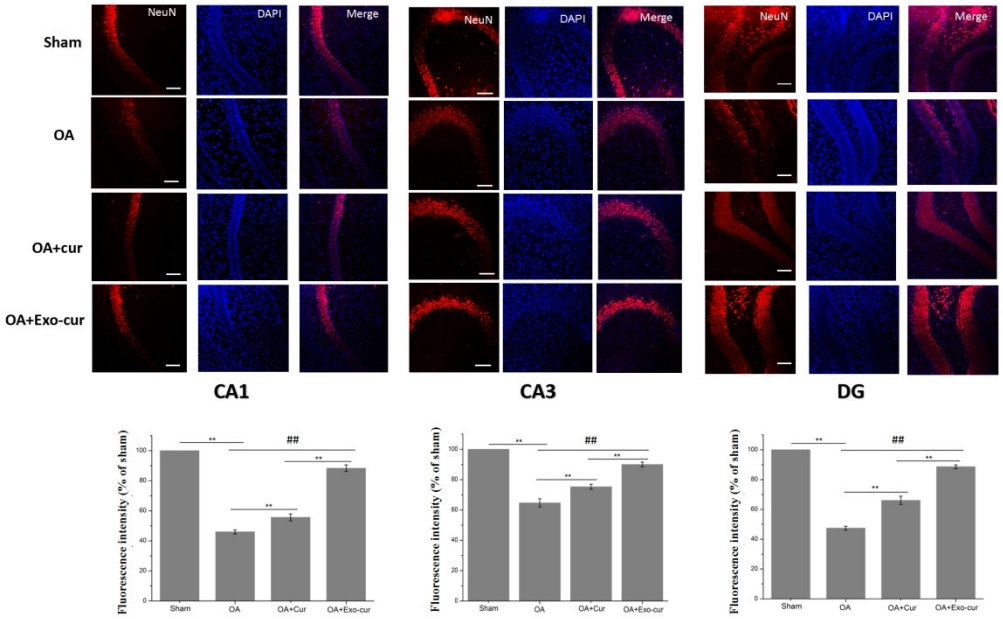

Fig. 6 Representative immunofluorescence staining for Neuron positive cells in hippocampal CA1 region, CA3 region and DG region after 7 days of daily peritoneal injection of free-cur and Exo-cur. NeuN antibodies were used to stain neurons in the hippocampus. DAPI (blue) was used as a nuclear marker. The scale bar is 100 μm and applies to all figure parts. Data are expressed as means ± SD (n=3). ** P < 0.01,## indicating P<0.01, compared OA+Exo-cur group with OA group.

View Article Online
DOI: 10.1039/C9NR01255A

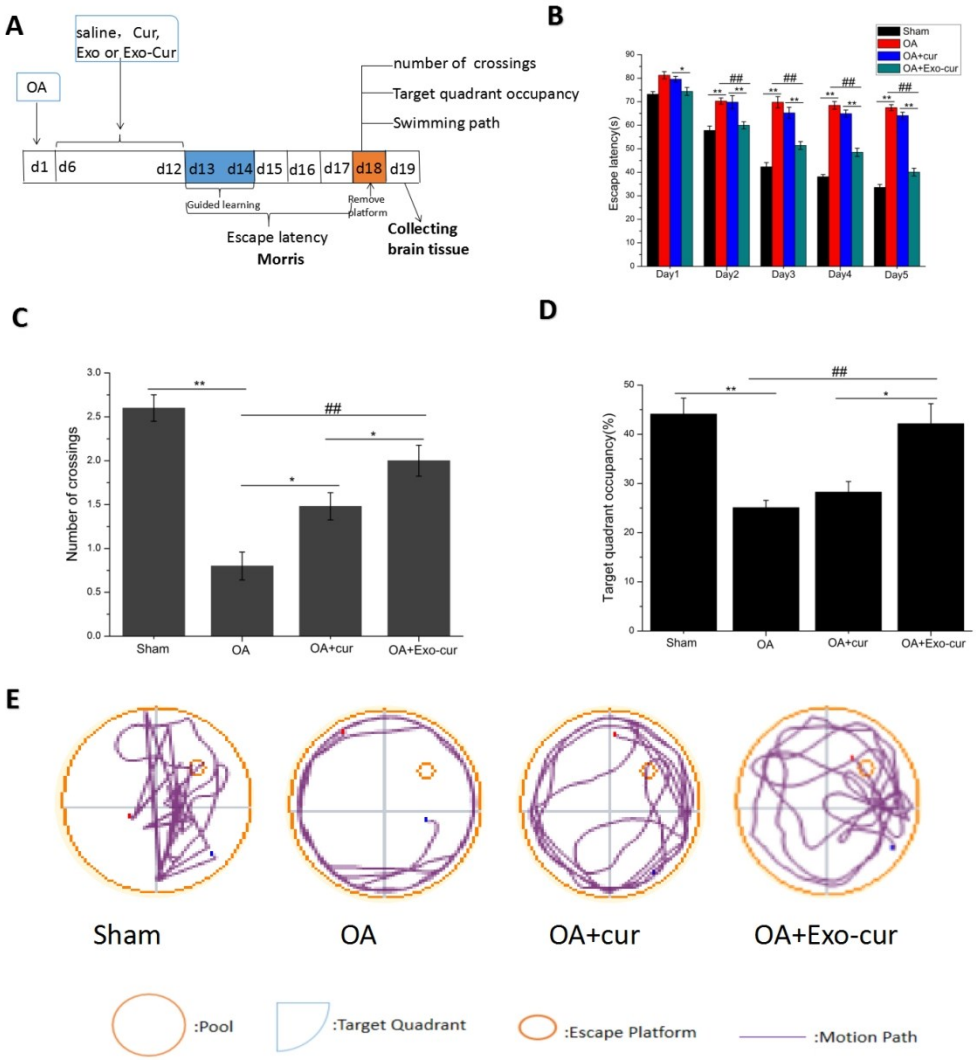

Fig. 7 Exo-cur ameliorates the cognitive deficiency in OA treated mice. (A) Experimental design for the animal study. (B) Escape latencies.analysis. Data are expressed as means ± SD (n=3). * P < 0.05, ** P < 0.01,## indicating P<0.01, compared OA+Exo-cur group with OA group. (C) The platform crossing number in the spatial probe test. Data are expressed as means ± SD (n=3). * P < 0.05, ** P < 0.01,## indicating P<0.01, compared OA+Exo-cur group with OA group. (D) Relative time percentage spent on the target quadrant in a probe trial. Data are expressed as means ± SD (n=3). * P < 0.05, ** P < 0.01,## indicating P<0.01, compared OA+Exo-cur group with OA group. (E) Representative path tracings of different groups.

View Article Online
DOI: 10.1039/C9NR01255A

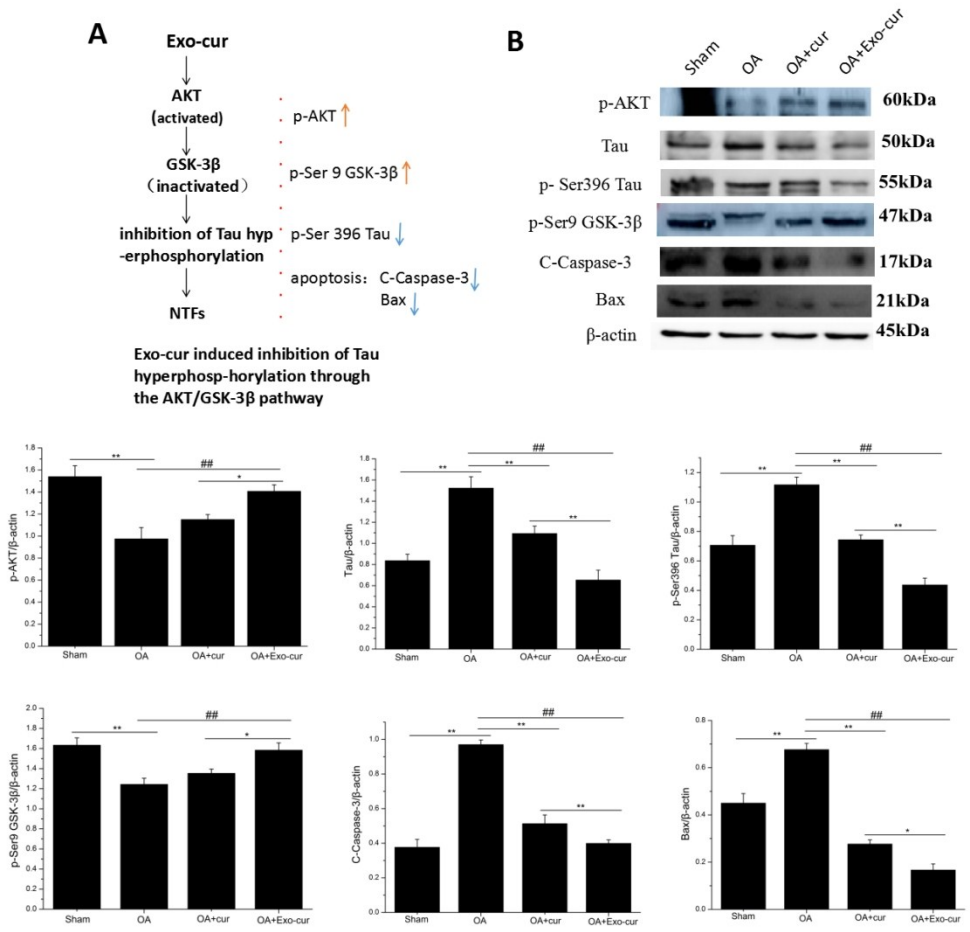

Fig. 8 In vivo therapeutic mechanism of Exo-cur in OA induced AD mice model. (A) A proposed model illustrating the mechanism underlying the efficiency of Exo-cur in the amelioration of cognitive impairment in AD. Exo-cur rescued neuronal cells from apoptosis by regulating pro-apoptotic proteins. Moreover, Exo-cur also inhibited Tau phosphorylation by activating AKT/GSK-3β pathway. (B) Western blot and quantification results of p-AKT, Tau, p-Ser396 Tau, p-Ser9 GSK-3β, Bax and C-Caspase 3 in hippocampus of OA induced AD mice after treatment with free cur and Exo-cur. Data are expressed as means ± SD (n=3). * P < 0.05, ** P < 0.01,## indicating P<0.01, compared OA+Exo-cur group with OA group.

467x456mm (72 x 72 DPI)

View Article Online
DOI: 10.1039/C9NR01255A

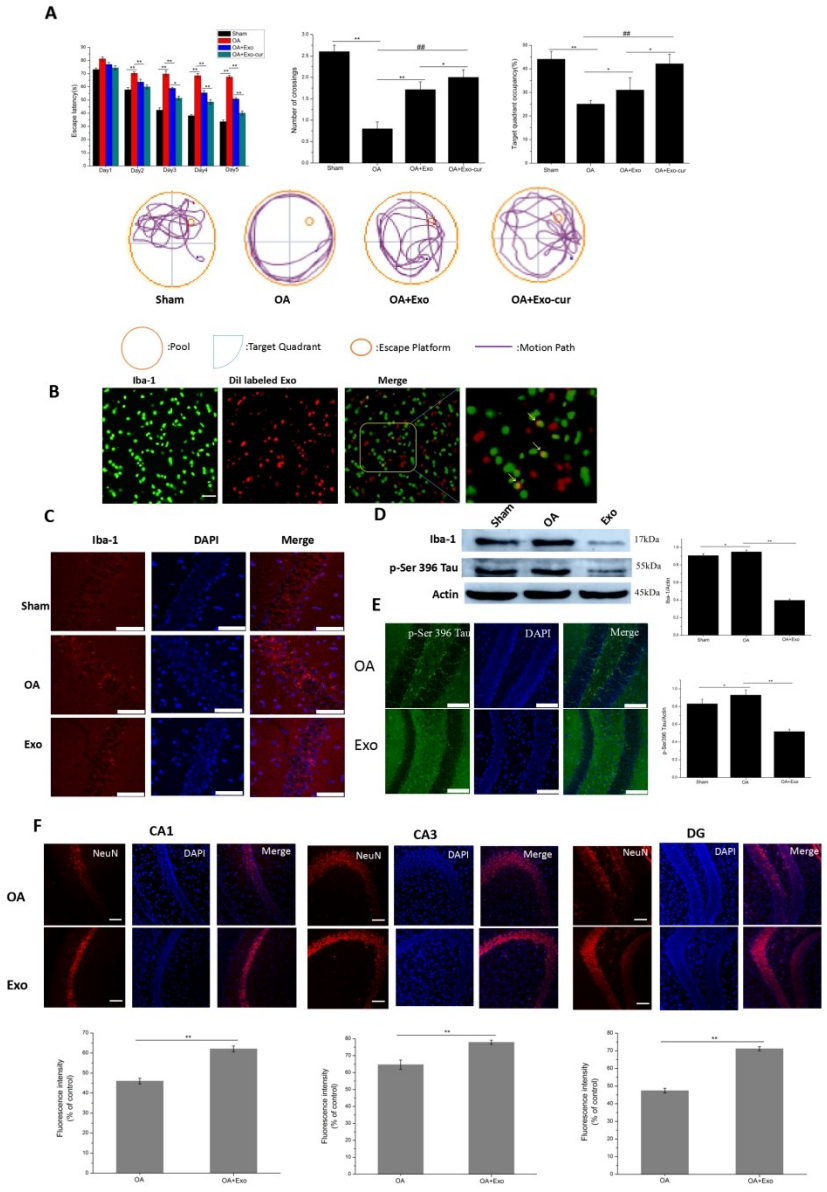

Fig. 9 Naïve Ex attenuates OA-induced cognitive decline in AD mice by relieving over-activation of microglia and reducing OA induced apoptosis of neuronal cells. (A) Hidden platform learning histograms. Subsequent histograms represent average of all daily trials. Data are expressed as means ± SD (n=3). *p < 0.05, **p < 0.01, ## indicating P<0.01, compared OA+Exo-cur group with OA group.(B) Co-location of DiI-labeled Exo with microglia cells in hippocampus of OA induced AD mice. Microglia was stained with anti-Iba1 (green). The scale bar is 50 μm and applies to all figure parts. (C) Brain tissues were fixed and stained with Iba-1 antibody, then imaged by immunofluorescence confocal microscopy (red). Nuclei were stained with DAPI (blue). Representative image demonstrating the morphology of microglia in hippocampus. The scale bar is 50 μm and applies to all figure parts. (D) Western blot results of Iba-1 and p-Ser396 Tau in hippocampus of OA induced AD mice after treatment with Exo. Data are expressed as means ± SD (n=3). *p < 0.05, **p < 0.01. (E) Representative immunofluorescence staining of p-Ser396 Tau in hippocampus of OA induced AD mice after treatment with Exo. DAPI (blue) was used as a nuclear marker. The scale bar is 100 μm and applies to all figure parts. (F) Representative immunofluorescence staining for Neuron positive cells in hippocampal CA1 region, CA3 region and DG region after peritoneal injection of Exo. NeuN antibodies were

View Article Online
DOI: 10.1039/C9NR01255A

used to stain neurons in the hippocampus. DAPI (blue) was used as a nuclear marker. The scale bar is 100 μm and applies to all figure parts. Data are expressed as means ± SD (n=3). **p < 0.01.

636x918mm (72 x 72 DPI)

View Article Online
DOI: 10.1039/C9NR01255A

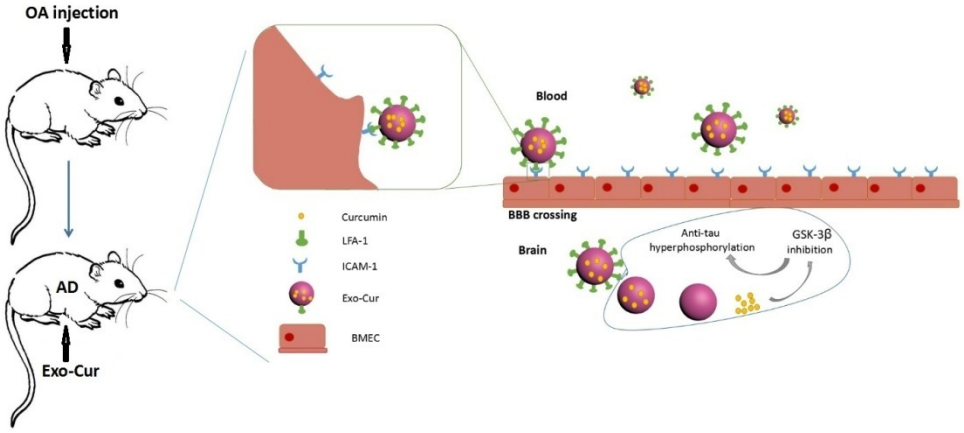

Curcumin-primed exosomes (Exo-Cur) can better relieve the symptoms of AD by inhibiting phosphorylation of Tau protein through AKT/GSK-3β pathway.

514x248mm (72 x 72 DPI)